Evaluation of the Candidate Models for IGRF-2010

Nils Olsen

DTU Space, Juliane Maries Vej 30, 2100 Copenhagen, Denmark

Draft, November 23, 2009

1   On the weighting of the candidate models

Traditionally, the final IGRF model was determined as the (weighted) arithmetic mean of the candidate models, with weights given to the candidate models rather than to the individual Gauss coefficients. As a consequence, all coefficients of a certain model was given the same weight. However, all coefficients of a model that for instance has deficiencies at polar latitudes have been downweighted, despite of the fact that some coefficients (for instance the tesseral coefficients) may be much less affected than the zonal coefficients, and thus should be weighted differently.

Such an individual weighting of the coefficients is cumbersome if the weights are to be found manually. However, this time we have seven candidate models for DGRF-2005 and IGRF-2010, and 8 candidate models for the SV for 2010-2015, which allows for applying statistical methods to weight the individual coefficients.

I therefore suggest to use a robust mean instead of an arithmetic mean (with pre-described weights). Since this is a well-defined way of degerming weights it will also help to decrease the subjectivity in choosing the weights for candidate models. (There is of course some freedom in the choice of the robust weighting function, for instance whether to use Huber weights, Tuckey's bi-weight, or some form of a trimmed mean).

In following I will present the results obtained by using Huber weights (with tuning constant $c = 1.5$).

From the seven candidate models for DGRF (i.e. 7×195 Gauss coefficients I calculated the Huber mean model. As part of this process a weight is assigned to each Gauss coefficient of each model (i.e. 7×195 weights are determined). The same procedure is applied to the seven candidate models for IGRF, and to the 8 candidate models for the SV. The robustly determined mean models are available at http://www.space.dtu.dk/˜nio/IGRF-evaluation/.

Figures 1 to 3 show the weights given to the various coefficients of the different models. The numbers on the abscissa $(1, 4, 9, 16, \ldots)$ indicate the weights given to the zonal coefficients $g_n^0, n = 1, 2, 3, \ldots$.

The following table presents the mean values of the weights given to the various candidate models by the Huber weighting scheme; note that these numbers are not recommended for assessment of all parts of a candidate model. Also listed are the numbers of downweighted coefficients ($w < 1$) for each candidate model.

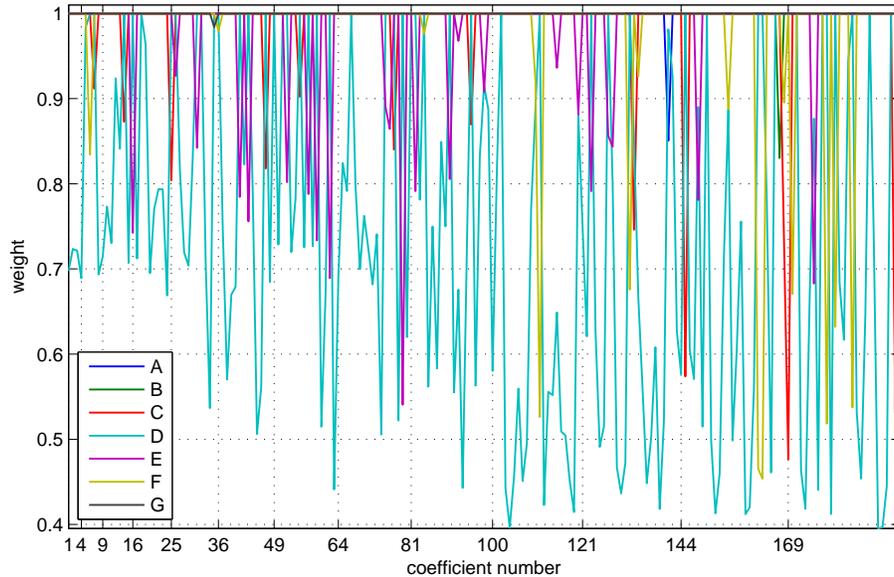| candidate	A	B	C	D	E	F	G	H
mean weights, IGRF	0.9992	0.9991	0.9850	0.7449	0.9775	0.9790	0.9999	
# $w < 1$	1	1	12	142	24	15	1	
mean weights, DGRF	0.9963	1.0000	0.9899	0.8158	0.9339	0.9950	0.9953	
# $w < 1$	4	0	13	101	60	12	4	
mean weights, SV	0.9746	0.9994	0.9868	1.0000	0.8239	0.9949	0.8688	0.9946
# $w < 1$	9	1	5	0	37	3	29	2

Figure 1: Weights given by the Huber weighting scheme to the coefficients of the different candidate models for DGRF 2005.

In conclusion: This analysis confirms some of the findings already reported by other groups regarding deficiencies of some candidate models. The most obvious examples are the DGRF and IGRF candidates of team D, but interestingly the SV candidate model of that group has been given the highest score by the Huber weighting scheme.

A final remark on the weighting: It has been suggested by Vincent Lesur to perform the weighting of the candidate models in the physical (spatial) domain rather than in the spherical harmonic domain. Such an approach would be useful
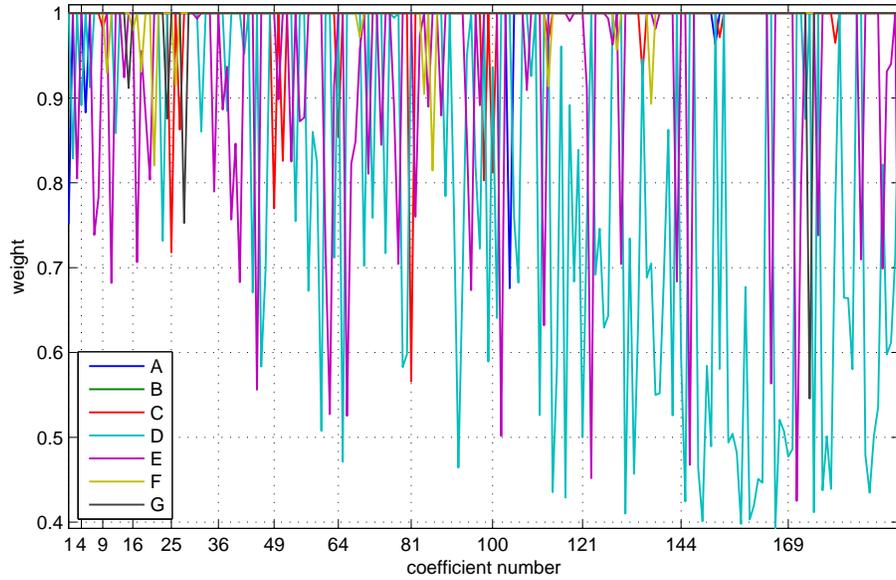
Figure 2: Weights given by the Huber weighting scheme to the coefficients of the different candidate models for IGRF 2010.

if the deficiencies of candidate models are restricted to certain geographical regions, for instance the polar areas, which would be the case if these models were affected by polar ionospheric currents. However, if the problem is due to contamination of magnetospheric sources (which mainly affects the degree-1 coefficients of the model, and especially g_1^0) it is more appropriate to perform the weighting in the spherical harmonic domain.
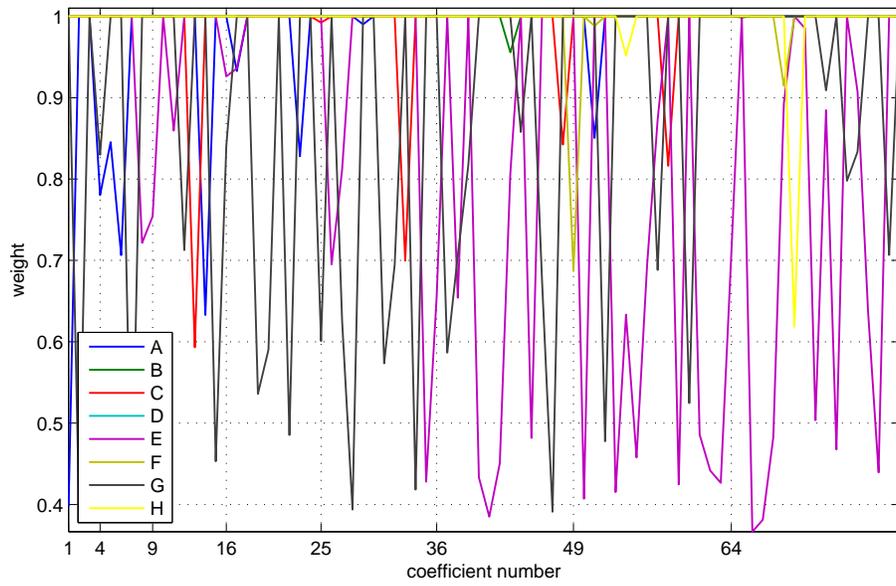
Figure 3: Weights given by the Huber weighting scheme to the coefficients of the different candidate models for SV 2010-2015.

2 Assessment of the candidate models for IGRF-2010 with CHAMP vector data

We compare the seven candidate models for IGRF-2010 with independent CHAMP satellite observations taken on October 17-20, 2009. These are four days of extremely quiet geomagnetic conditions, as shown in Figure 4. Unfortunately, by mid-November, when this evaluation was done, no finally aligned CHAMP vector data ("Level 51") were available from the CHAMP data center ISDC. Only preliminary data were available, and use of these data reveals large-scale residuals of order 10 nT, which are typical values for data that are not finally aligned. (Alignment is the process of rotating the vector data from the magnetometer frame to the star imager frame.)
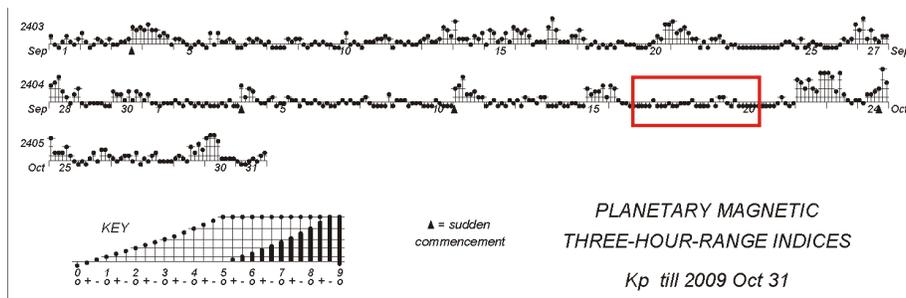

Figure 4: Geomagnetic activity in October 2009 as measured by the Kp index. With red are marked the four days that have been used for the evaluation.

CHAMP alignment parameters (Euler angles) are determined as part of the CHAOS field-modeling effort, and we used the Euler angles that have been determined for October 2009 from an update of the CHAOS-3 model to align the CHAMP vector data for our assessment.

To make the assessment we applied the following steps:

- Only the night-side part of the CHAMP orbits are used, and data are subsampled every 10 secs (local time of CHAMP is about 04:00/16:00 during those days).

- The crustal field part of CHAOS-3 (degrees $n = 14 - 39$) are removed from the CHAMP data

- The external field model of xCHAOS is removed (model family, although I do not expect significant changes when using external coefficients from a more recent model), but using a value of $q_1^0 = -6.5$ nT (which is the mean of the values determined for 2009 by CHAOS-3).

- All candidate models are propagated from epoch 2010.0 to epoch 2009.80 (October 18, 2009) using the robust mean SV model described in the previous section. Synthetic main field model values $\mathbf{B}_{\mathrm{MF}}$ are then calculated

5

model	ΔB_r		ΔB_θ		ΔB_ϕ	
	mean	rms	mean	rms	mean	rms
A	-1.67	5.17	-3.88	11.77	2.90	10.39
B	-2.39	5.69	-1.98	11.83	2.88	10.38
C	-3.45	6.59	-1.01	11.51	2.84	10.62
D	-3.05	8.61	-1.52	12.15	2.90	11.09
E	-2.62	7.57	-2.03	13.21	2.87	10.45
F	-1.78	5.59	-2.43	12.08	2.93	10.36
G	-2.38	6.00	-1.82	11.80	2.85	10.65

Table 1: Statistics of residuals at non-polar latitudes (13275 vector triplets equatorwards of $\pm 55°$ dipole latitude).

for each candidate model, and subtracted from the observations to obtain the vector residuals $\Delta\mathbf{B} = \mathbf{B}_{\text{obs}} - \mathbf{B}_{\text{ext}} - \mathbf{B}_{\text{crust}} - \mathbf{B}_{\text{MF}}$.

Figures 5 and 6 show the residuals $\Delta\mathbf{B}$ in dependence on dipole latitude for the three components ΔB_r (left), ΔB_θ (middle) and ΔB_ϕ (right) and all seven candidate models. Maps of the residuals are presented in Figure 7.

Tables 1 and 2 list arithmetic mean and rms of the residuals, for non-polar and polar latitudes, respectively. ΔB_ϕ at polar latitudes is very much affected by the contribution from local field-aligned currents and is therefore less suited for assessment of the candidate models.

model	ΔB_r		ΔB_θ		ΔB_ϕ	
	mean	rms	mean	rms	mean	rms
A	-5.66	10.09	-2.50	13.89	-0.30	21.20
B	0.61	8.18	-2.66	14.32	-0.18	21.09
C	15.73	21.42	6.64	15.71	0.03	21.20
D	-8.14	16.40	-7.76	18.39	-0.23	22.12
E	10.95	16.17	2.10	16.72	-0.11	21.84
F	-2.65	10.21	-5.02	15.17	-0.33	21.09
G	-1.39	9.15	-4.51	14.96	-0.06	21.30

Table 2: Statistics of residuals at polar latitudes (3620 vector triplets polewards of $\pm 55°$ dipole latitude).
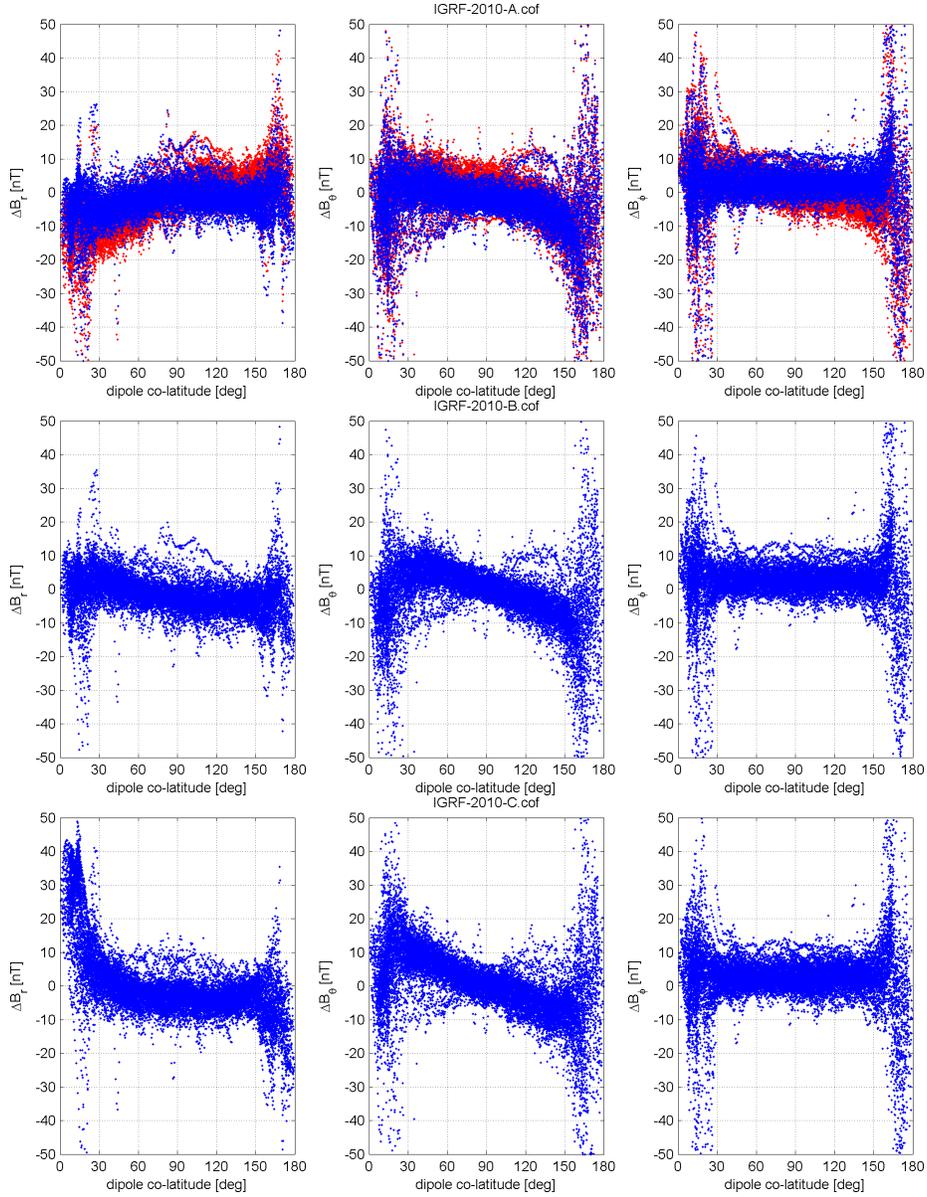
Figure 5: Residuals in dependence of dipole latitude for the first three (out of seven) candidate models A (top) to C (bottom). The red symbols in the top panel (model A) represent residuals hat have not been corrected for external field contributions. They are shown to illustrate the benefit of a correction for external fields.
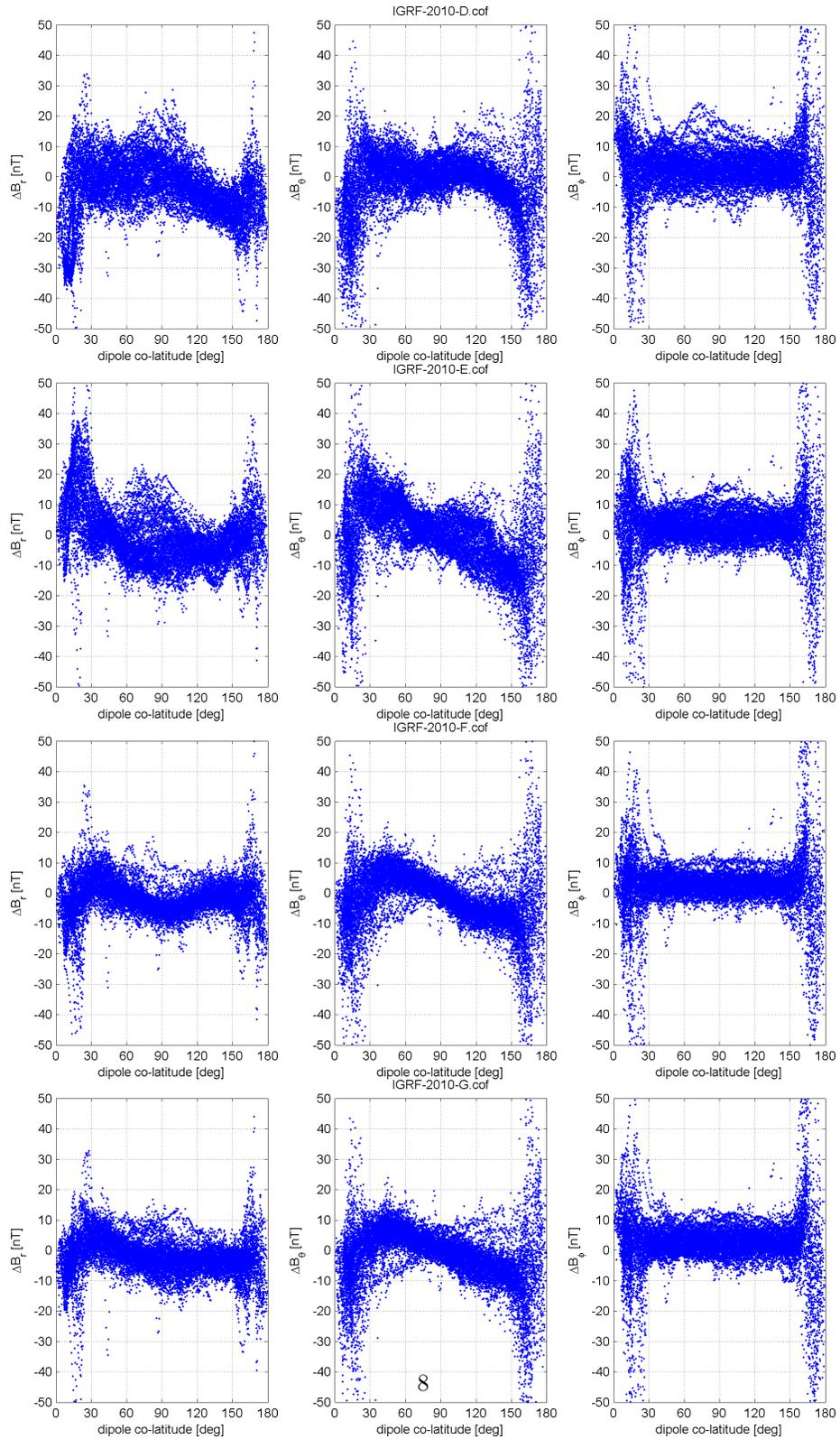
Figure 6: Residuals in dependence of dipole latitude for the last four (out of seven) candidate models D (top) to G (bottom).
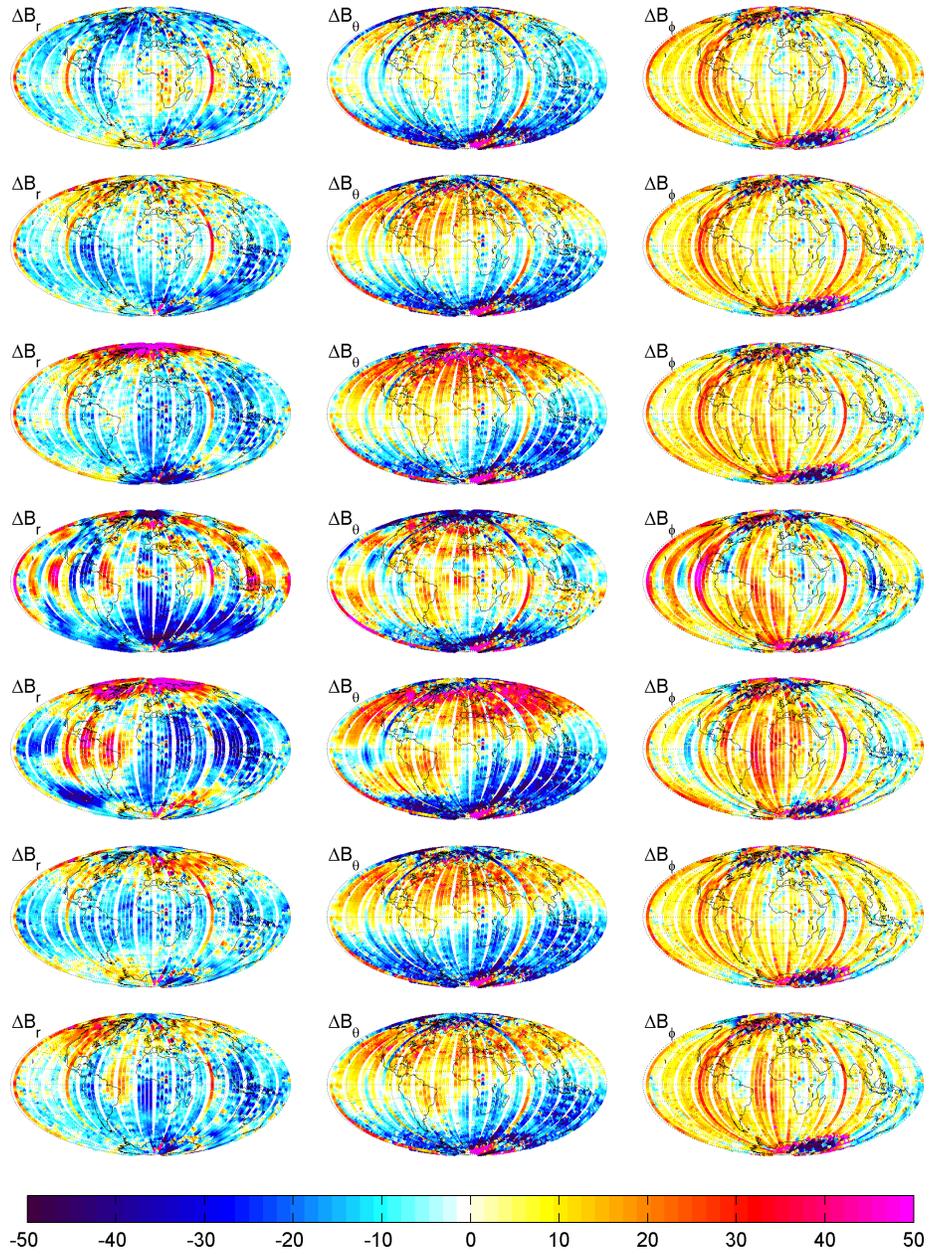
Figure 7: Maps of CHAMP Residuals (in nT), after removal of crustal field (for $n = 14 - 30$) and external field, for the 7 candidate models A (top) to G (bottom).